Laser floating zone growth of Yb, or Nd, doped $(Lu_{0.3}Gd_{0.7})_2SiO_5$ oxyorthosilicate single-crystal rods with efficient laser performance

F. Rey-García[*a,b], F. M. Costa*[c] *, and C. Zaldo*[†d]

[a]Instituto de Ciencia de Materiales de Aragón. Consejo Superior de Investigaciones Científicas. c/ María de Luna 3. 50018 Zaragoza. Spain.

[b]Unidad Asociada de Microóptica y Óptica GRIN. Universidade de Santiago de Compostela. c/ Campus Sur s/n. 15782 Santiago de Compostela. Spain.

[c]Departamento de Física & I3N. Universidade de Aveiro. 3810-193 Aveiro. Portugal.

[d]Instituto de Ciencia de Materiales de Madrid. Consejo Superior de Investigaciones Científicas. c/ Sor Juana Inés de la Cruz 3. 28049 Madrid. Spain.

Email: [†]cezaldo@icmm.csic.es *francisco.rey.usc@gmail.com,

ABSTRACT

Disordered crystals are being presently developed to enlarge the fluorescence bandwidths of trivalent lanthanides incorporated for generation of ultrashort (femtosecond) laser pulses in mode-locked oscillators and amplifiers, but crystal disorder induces a reduction of the thermal conductivity which hampers the uniform crystal cooling after growth, leading to internal stresses. This is particularly remarkable when using the Laser Floating Zone (LFZ) growth technique, thus so far laser operation has been obtained only for LFZ-grown crystals with high thermal conductivity ($\kappa \geq$ 10 W/mºC) but without disorder, i.e. YAG, Y_2O_3 or $REVO_4$. To overcome this limitation we present the LFZ growth of $(Lu_{0.351}Gd_{0.630}Yb_{0.019})_2SiO_5$ and $(Lu_{0.307}Gd_{0.612}Nd_{0.081})_2SiO_5$ refractory (melting point ≈1950 ºC) oxyorthosilicates single crystal rods with dimensions suitable for high power diode laser pumping, despite these crystals have medium/low thermal conductivity, $\kappa <$ 4 W/mºC. Rods with ≈10 mm length and ≈1.75 mm of diameter were grown in air under a CO_2 laser at 10 mm/h. X-ray diffraction analyses confirm the monoclinic *C*2/*c* structure of the obtained crystals. For the chosen ≈0.3Lu/0.7Gd ratio some of the crystals are transparent and free of macro-defects. The continuous wave laser performance of Yb^{3+} and Nd^{3+} incorporated ions is demonstrated under Ti-sapphire laser pumping in an astigmatism compensated z-shaped optical cavity. Laser performance of these LFZ oxyorthosilicates is found comparable to that reported in Czochralski (Cz) grown crystals. The faster pulling rate (almost one order of magnitude larger for LFZ than for Cz), the high crystal composition purity, and the absence of crucible or atmosphere control make the LFZ technique a low cost alternative for the present needs of diode laser pumped mode-locked medium/high power laser oscillators.

Keywords: Laser Floating Zone. Refractory crystal growth. LGSO oxyorthosilicate crystals. Disordered crystals. Lanthanide doped laser. Yb laser. Nd laser.

1. INTRODUCTION

Nowadays the development of robust, low cost, diode laser (DL) pumped and table top mode-locked fs laser systems with medium-high power (≈ kW) is attracting huge attention in order to transfer this technology from laboratory to industrial environments. In scientific laboratories and for academia applications these systems are based in titatium sapphire (Tisa) crystal, but the requirement of green light for Ti^{3+} pumping limits their power scaling and thus the transfer to industry. In this context Yb^{3+}- or Nd^{3+}-doped lasers resonantly pumped by DL at λ≈ 980 nm or λ≈ 810 nm, respectively, have arisen as an alternative to achieve the above purpose. [1-3]

Accordingly to the uncertainty quantum principle, the generation of ultrashort laser pulses requires optical amplification media with bandwidths (Δν) complying the time-bandwidth product law, which for Gaussian pulses of duration τ is written as Δν×τ= 0.441. The d^1 electrons of Ti^{3+} have a strong interaction with the vibrating crystal field leading to a very large band broadening, reaching typically Δν≈ 160 THz (λ≈ 650-1000 nm) which supports sub 10 fs laser pulse durations. However, trivalent lanthanide (Ln^{3+}) optical spectroscopy is related with intraionic f^n-f^n electronic transitions, and 4f orbitals are shielded by the outer 5s and 5p ones, as result, absorption and emission bands of Ln^{3+} are spectrally much narrower than those observed in transition metal ions. Although Yb^{3+} with the nearly filled f^{13} shell exhibits broader bands than other Ln^{3+}, its fluorescence bandwidth is still rather small, Δν≈ 27 THz (λ≈ 1010-1080 nm). These narrow bands are not convenient to match thermal drifts of the pumping DL (typically 0.25-0.4 nm/ºC) and compromise the sustainability of sub 100 fs laser pulse durations. For this reason a large number of single-crystal hosts are nowadays being tested for mode-locked lasers with pulse duration below 100 fs, and particularly the so called "disordered" crystals. The latter are crystalline hosts either with multiple sites for the Ln, with Ln surrounding lattice positions shared by several different cations or with structural point defects (e.g. vacancies, interstitials, etc). In these cases the Ln bands are inhomogeneously broadened helping to overcome the above mentioned spectral bandwidth limitation of Ln^{3+}.

In this search for new crystalline laser hosts, refractory oxides with high melting temperature are receiving particular attention because their growth is little developed with the exception of some few standard solid state laser (SSL) hosts (e.g. $Y_3Al_5O_{12}$ garnet, YAG). These oxides have ionic character chemical bonds what makes them chemically stable but the availability of proper crucibles is one important limitation for the growth of such refractory crystals. Up to ≈ 1500 ºC platinum is used in air atmosphere. For higher temperature, iridium (melting at 2446 ºC) is used but an oxygen poor atmosphere is required to avoid crucible oxidation, thus the as-grown crystals often exhibit color defects and Ir inclusions. Some crystals of great interest as laser host melt even at higher temperature, for instance Sc_2O_3 and Lu_2O_3 melt at 2485 and 2490 ºC, respectively, requiring even more fragile crucibles, e.g. molybdenum or tungsten (melting at 2630 ºC or 3422 ºC, respectively). Thus, either fluxes to reduce the melting temperature or crucible-less (Verneuil, floating zone, etc) crystal growth techniques must be assay for new developments and processing of laser crystals.

Laser floating zone (LFZ) crystal growth technique, also known as laser-heated pedestal (LHP) method, is a crucible-less technique often used for the growth of optical, magnetic or superconductor crystals. [4,5] Regarding laser applications, pioneering work on Nd-doped YAG,[6] and Y_2O_3 [7] optical fiber preparation was made by Stone and coworkers in the middle of 1970´s by material melting with a CO_2 laser, the diameter of these fibers was in the 50-100 μm range with lengths up to 3 cm, laser effects in these confined media were qualitatively demonstrated. These thin fibers are not suitable for the presently used high power DL pumping since the laser emission is delivered through optical fibers with large (100-300 μm) core diameters what requires material cross sections in excess of 1 mm^2. Further prospective work also using a CO_2 laser for the LFZ growth of optical single-crystal oxides was made in the late 1980´s by de la Fuente and coworkers [8,9] and by Tissue and coworkers, [10] although structural and spectroscopic studies were reported, no laser demonstration was presented in these studies. Afterwards the technique was applied by Erdei to obtain rare earth (RE) $REVO_4$ vanadates melting at ≈ 1810 ºC,[11] and after about ten years of crystal growth development a variant of this technique (heating with 1.5 kW halogen lamps, known as Optical Floating Zone, OFZ, method) produced Nd-,[12], Er-,[13] Tm-,[14] and Yb-[15] doped $REVO_4$ crystals with good laser efficiency. Nd-doped $YAlO_3$ (YALO) LFZ grown crystals have been also assessed as laser SSLs.[16]

Although LFZ growth technique has been used to produce single-crystals of a large number of materials with optical applications (including potential lasers), laser action has been demonstrated only in few of them, basically in those having large thermal conductivity (κ): YAG (κ≈ 11 W/mºC), Y_2O_3 (κ≈ 13.4 W/mºC), YALO (κ≈ 10-13.3 W/mºC) and $REVO_4$ (κ≈ 10 W/mºC) crystals. [17,18] The application of the LFZ technique to the growth of defect-free transparent

single-crystals of materials with lower thermal conductivity has been challenging due to large axial and radial thermal gradients associated to the irradiation geometry and possible contamination with undesired phases formed by the reaction of the precursor compounds. The requirement of crystalline disorder is one added difficulty for the crystal growth because the simultaneous introduction of ions with different masses reduces the thermal conductivity.[19] YAG and $REVO_4$ are ordered crystals with a unique crystallographic site for the RE, although some inhomogeneous band broadening can be achieved in these compounds by mixing of REs with different ionic sizes (Y or Lu versus Gd), this leads to the afore mentioned reduction of thermal conductivity and even phase modifications hampering the LFZ growth of crystals suitable for lasing, thus the growth of alternative disordered crystals is required.

Rare earth (RE= Y, Sc or Ln) oxyorthosilicates with chemical formula RE_2SiO_5 (hereafter shorten as RESO) as well as RE= Sc/Y, Y/Ln and LnA/LnB mixed ones are disordered crystals that have been extensively studied earlier for scintillating purposes, thus the fundamental physical properties and growth-related chemistry are relatively well known. They melt in the 1950-2000 ºC range depending on composition,[20] their crystalline structure is monoclinic being optically positive biaxial crystals, but the crystallization space group depends on their atomic constituents. Oxyorthosilicates with large trivalent RE ionic radius, such as Gd_2SiO_5 (GSO), crystallize in the monoclinic $P2_1/c$ space group with two crystallographic sites for the gadolinium, Gd1 (9-fold oxygen coordinated) and Gd2 (7-fold oxygen coordinated) but crystals with this structure are prone to cleavage along the (100) plane, which limits laser power scaling. In spite of this limitation medium power cw (< 3W with 49% slope efficiency) [21] and pulsed mode-locked (343 fs of pulse duration/ 396 mW average power) [22] DL pumped Yb lasers have been demonstrated with Yb:GSO crystals.

Oxyorthosilicates with small RE^{3+} ionic radius, such as Y_2SiO_5 (YSO),[23] Sc_2SiO_5 (SSO),[24] and Lu_2SiO_5 (LSO),[25] crystalize in the monoclinic $C2/c$ space group. This crystallographic structure presents two sites, RE1 and RE2, with 6+1-fold (the extra oxygen is not bonded to other cations) and 6-fold oxygen coordination, respectively, linked by SiO_4 tetrahedra forming chains further linked together by SiO_4 polyhedra. This latter crystalline structure lacks of easy cleavage, thus it is more appropriated for high power laser applications, and in fact, it has attracted great attention for this purpose due to the very large crystal field intensity on Yb^{3+} in this host. The $^2F_{7/2}$ splitting of the fundamental Yb^{3+} multiplet of the RE2 site (with very short average RE-O bond length, 2.23 Å) reaches 1012 cm^{-1},[26] being one of the largest known, what largely reduces the emission reabsorption problem of this quasi-three level laser and thus reduces the laser pump threshold. These oxyorthosilicates were initially considered as crystals with intermediated thermal conductivity κ= 4.4-5.3 W/mºC, [25] but this view may be less positive to the light of new measurements that reduce these values to κ= 2.26-3.67 W/mºC for LSO. [27] The incorporation of laser active Ln may influence the crystalline structure depending on the ionic radius and amount of incorporation. Mixed $(LnA_{1-x}LnB_x)_2SiO_5$ crystals have been developed to improve the optical quality of Czochralski (Cz) grown crystals [20] and to accommodate laser Ln with different ionic sizes, from Pr^{3+} to Yb^{3+}.

Single-crystals of all the above oxyorthosilicate compositions have been grown by the Cz method using Ir crucibles in high purity 99.99% N_2 atmosphere at a pulling rate of ≈1 mm/h. As a result of this extensive activity cw and mode-locked laser operation have been demonstrated. YSO, LSO, SSO, as well as Lu/Gd (LGSO) and Y/Gd (YGSO) have been studied extensively as cw Nd, [28-30] Tm,[23] and Yb [31-34] SSLs. Furthemore, mode-locked laser pulses as short as 54 fs (average output power 25 mW, λ= 1052 nm, repetition rate 113 MHz) have been demonstrated by Kerr-Lens mode-locking with Yb:LSO Cz single-crystals [35] and 122 fs pulses (410 mW, λ=1041 nm, 75 MHz) using a semiconductor saturable absorption mirror (SESAM) as pulsing element.[36] All this laser related activity is so far restricted to Cz-grown crystals. Moreover, Ln= Ce, Pr, Sm, Eu, Tb, Tm and Yb-doped LSO crystals have been grown by the OFZ technique using 1.5 kW halogen lamps in N_2 atmosphere, but these crystals were only used for optical spectroscopic (radioluminescence and scintillation) characterizations.[37,38]

We have recently explored the LFZ growth of several transparent oxides with congruent melting [39] and we have found that oxyorthosilicates could be appropriated for laser purposes. In our previous LFZ attempts to grow oxyorthosilicates, we have first evidenced that GSO crystalline rods exhibit a yellowish color, transversal cracks and internal small defects that could not be avoided even when the crystallization rate was reduced from 100 mm/h to 10 mm/h.[40] On the other hand, LFZ attempts to produce LSO led to an eutectic ceramic where monophasic LSO regions are alternated with biphasic LSO/Lu_2O_3.[41] So, these simple approaches do not yield crystals suitable for laser applications. However, Lu/Gd mixed oxyorthosilicates obtained by LFZ have few defects and look transparent, particularly for the $(Lu_{0.3}Gd_{0.7})_2SiO_5$ composition,[42] and they are able to accommodate the small Y^{3+} ion without degradation of optical properties or crystallographic phase changes.[43] In the present work we have used the above

optimized Lu/Gd composition to host small (Yb^{3+}) and large (Nd^{3+}) ionic radius laser lanthanides and for the first time to our knowledge we present laser operation in a LFZ grown oxyorthosilicate.

2. EXPERIMENTAL TECHNIQUES

2.1 Crystal growth

$(Lu_{0.3}Gd_{0.7})_2SiO_5$ oxyorthosilicate crystalline rods nominally doped with 5 mol% of Yb^{3+} (Yb:LGSO) or Nd^{3+} (Nd:LGSO) were grown by the LFZ technique. Figure 1 sketches the used equipment and Table 1 summarizes some of the growth parameters. Heating is provided by the absorption in the precursor rod of the 200 W CO_2 laser (Spectron, GSI group) emission. The laser beam is expanded and shaped by a set of four gold coated mirrors. The reflaxicon is formed by a first inner conical mirror that expands the CO_2 laser beam and a second outer conical mirror that recollimates it producing a circular crown-shaped laser beam, which size is defined by rod cylinder diameter. [41] The 45 degrees titled plane mirror redirects the laser beam vertically and the last parabolic mirror concentrates the laser energy on the rod´s surface generating a floating zone configuration with uniform radial heating. Although not essential, a chamber is used to confine the laser radiation avoiding undesired reflections in the room. A ZnSe window is used for the laser entrance to the chamber. This chamber also has mechanical accesses for the rotation and vertical displacement of the precursor rod. All growth experiments were made in air at room conditions.

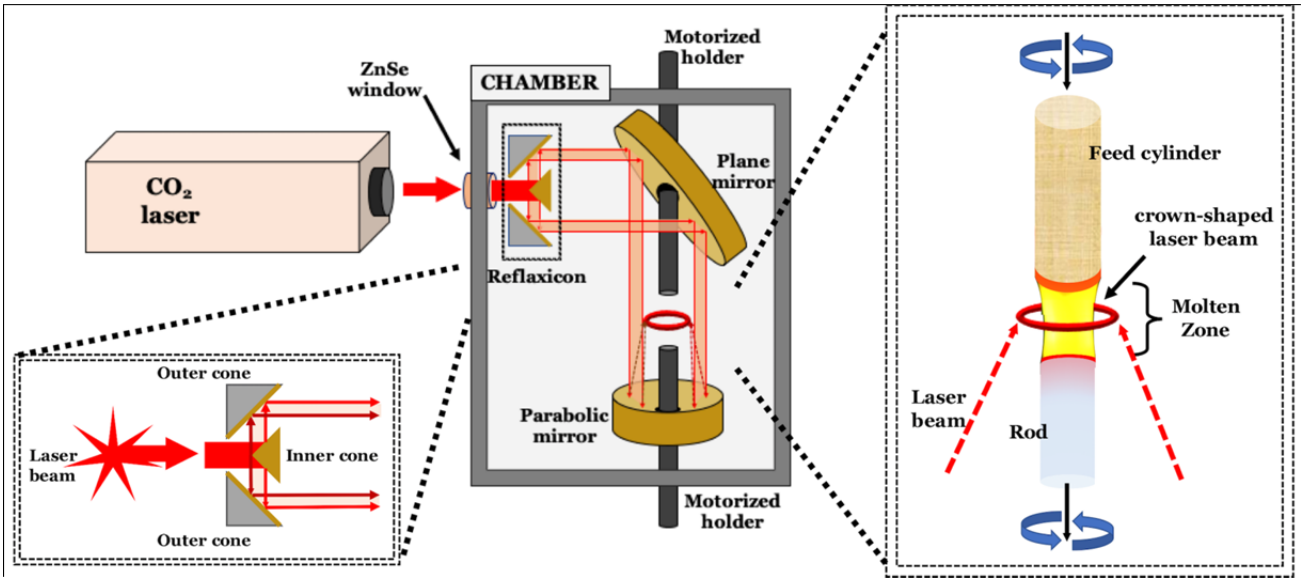

Figure 1. Crystal growth used setup. The left inset show the “reflaxicon” operation and the right inset shows the light focusing on the processed precursor polycrystalline feed cylinder and the obtained single-crystal rod.

The precursor feed cylinders for the LFZ growth were prepared by mixing in an agate ball mill, 3h at 200 rpm, commercial powders of Gd_2O_3 (MaTeck, 99.999%), Lu_2O_3 (Shangai Co., 99.99%), SiO_2 (Aldrich, 99.99%) and Yb_2O_3 (MaTeck, 99.999%) or Nd_2O_3 (MaTeck, 99.999%). The milling homogenizes the feed cylinder composition and substantially reduces particle size of the precursor oxides. This step plays a very important role in the LFZ crystal growth since it reduces the melting temperature and facilitates the diffusion of particles into the melt together with a better densification when they are later extruded. Powder oxide mixtures were bind by adding polyvinyl alcohol (PVA, Merck, 0.1 g/ml) and extruded into cylindrical rods with diameters about ≈2 mm. The precursor cylinders were firstly densified by pulling in the LFZ equipment at 100 mm/h under ≈87 W of CO_2 laser power (Table 1). These densified cylinders keep the desired composition and diameter, but exhibit a sort of macrostructural fractures that do not compromise integrity during the later processing. Some of these cylinders with better crystalline appearance were selected as seeds, while the rest were used as feed materials. Seed and feed rods were contacted and welded with the laser and final crystalline rods with diameters from 1.5 to 1.75 mm were grown in air at atmospheric pressure. Best results were

obtained moving the rod in the downwards direction at 10 mm/h of pulling rate under a rotation speed of 5 rpm and applying a CO_2 laser power of 83 W. In order to reduce internal stress in crystals due to the high temperature gradients present and the moderate thermal conductivity of the oxyorthosilicates, once a length suitable for laser performance studies was achieved, the temperature of the molten zone was decreased gradually by reducing the CO_2 laser power.

2.2 Composition analyses.

The Ln relative composition in the LFZ grown crystalline rods has been determined by X-ray fluorescence spectrometry using a JEOL electron microscope equipped with an electron probe micro analyzer, JEOL Superprobe JXA-8900 M. Polished samples were coated by evaporation with a thin carbon layer in order to avoid electric charge accumulation. Sexquioxide lanthanide standards were used for the analytical calculations performed with the equipment software. Results were averaged ten times on three different sample positions. Within the method accuracy (≈ 5%), no significant spatial composition variations were observed for the samples studied.

2.3 Structural characterization

The crystalline phase of the LFZ grown single-crystal rods has been assessed at room temperature (RT) by powder X-ray diffraction (pXRD). θ-2θ scans from 5 to 85 degrees were performed on a Bruker AXS D8 Advance equipment under Cu K_α radiation, and the Bragg diffracted light was collected by a Lyneye detector. For this purpose, the LFZ crystals were manually grinded in an agate mortar.

2.4 Laser characterization

Laser demonstrations were made by using a Z-shaped astigmatically compensated optical resonator pumped with a cw Spectra Physics Tisa laser, model 3900S. The Tisa laser was tuned at about 977 or 811 nm for pumping of Yb^{3+} or Nd^{3+}, respectively. The resonator is composed of two concave folding mirrors (reflectivity r > 99.9% for λ= 1010-1200 nm and r < 2% for λ= 800-985 nm) with radius of curvature RC= -100mm, a rear plane high reflector (r > 99.8% for λ= 800-985+1010-1200 nm) and a plane output coupler with transmission T_{OC}= 10% at the expected laser wavelength, λ= 1030-1100 nm. These optical elements were manufactured by Layertec.

The oxyorthosilicate crystalline rods were polished with two faces parallel to the growth direction. These uncoated samples were set at normal incidence between the two folding mirrors of the cavity and passively cooled with a Peltier system at 18 ºC. The Tisa laser beam was focused by a biconvex lens of focal distance f= 80 mm. This produces a beam waist diameter of 62 μm which matches well the calculated resonator mode size. The polarization of the Tisa laser was horizontal and the pumping beam was introduced into the resonator through a folding mirror. More details about the laser resonator and optical procedures can be found in a previous work. [44]

In order to determine the absorbed pump power the Fresnel sample reflection was estimated using an average refractive index n= 1.8, accordingly with the values reported in previous literature for isostructural LSO.[25,45,46] Laser powers were measured with Gentec photodetectors, model UP19K-15S-H5D0. The spectral distribution of the laser emissions was determined with an APE laser spectrometer, model Wavescan.

3. RESULTS AND DISCUSSION

3.1 Crystal growth

Figure 2 shows the Yb- or Nd-doped LGSO oxyorthosilicate rods with ≈0.3Lu/0.7Gd of nominal ratio successfully obtained by the LFZ growth technique. As-grown rods appear transparent in all cases. Yb-doped rods look colorless, Figure 2a, while those Nd-doped ones show the violet coloration typical for this ion, Figure 2d. The rods have a cylindrical geometry. The cross section diameter of single crystal rods ranges from 1.5 to 1.75 mm, depending on composition (see Figures 2a and 2b), i.e. ≈ 12% smaller than the densify precursor cylinder diameter. The observed rod diameter fluctuation relates on one side to uncertainties in the manual extruding processing of the precursor cylinders and on the other to the complexity to maintain the equilibrium of the contact angle [5] for the materials here considered. Also noting the higher diameters achieved here if we compare to laser fibers [6,7,10] ranging 50-700 μm.

Figures 2b, 2c, 2e and 2f show these rods after polishing. Yb-doped LGSO rods have most of their volume free of macrodefects or transversal cracks. Although Nd-doped LGSO rods also have large defect-free areas, the number of cracks and inclusions is obviously larger than in the Yb-doped cases. Moreover, in the Yb-doped rods it was easier to

maintain constant the diameter than in the Nd-doped ones. The latter shows diameter variations up to 25%. This behavior could be due to the different change of the crystal physical properties associated to the incorporation of lanthanides with ionic radius and mass different to those of the host. It is well known that substitutions with alike atomic mass induce a reduction of the crystal thermal conductivity,[19] making sample cooling more difficult, while larger ionic radius doping increases the lattice parameter and then it creates elastic stress in comparison to undoped material. Thus the relatively Nd^{3+} heavy doping, see later, with larger ionic radius and lighter atomic mass than Gd^{3+} or Lu^{3+} seems to have a more negative effect on the crystal quality than that of Yb^{3+} whose ionic radius and atomic mass are virtually identical to Lu^{3+}.

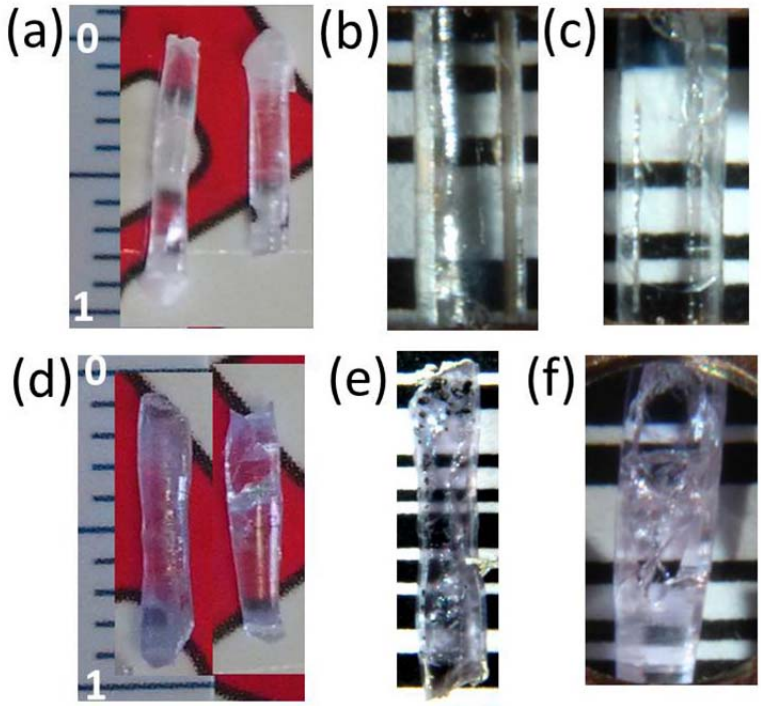

Figure 2. Pictures of a-c) Yb- and d-f) Nd-doped LGSO oxyorthosilicate rods grown by LFZ at a pulling rate of 10 mm/h with a rotation rate of 5 rpm. As-grown samples, a and d (scale in cm). b,c (rod diameter ≈ 1.4 mm) and e,f (rod diameter ≈ 1.7 mm) are samples with polished parallel faces.

Table 1 shows the composition of the obtained single-crystal rods as determined by the microprobe. It is worth noting that large deviations from the nominal compositions are not observed but in the case of the largest Nd^{3+} lanthanide some incorporation excess is observed (segregation coefficient >1) while in the case of the smallest laser active ion, Yb^{3+}, a clear compositional deficiency regarding the nominal composition (segregation coefficient <1) is observed, which is compensated by extra incorporation of Lu^{3+}. Such ionic size dependent segregation coefficient behavior is often observed in the growth of laser Ln-doped oxide single-crystals. [47] In both analyzed crystals the Gd composition is lower than nominal which agrees with the previous results obtained by EDX on isostructural LFZ crystals.[42]

The segregation coefficient of Nd in Czochralski grown crystals have been reported as 0.7 and 1 for YSO and GSO, respectively,[28] while in LGSO it was reported as 0.44. [29] In our case it has been determined to be 1.6. It seems apparent that the confinement of the material in a small melted volume favours to the Nd incorporation. On the other hand, the Yb segregation coefficient obtained in the present work, 0.37, is clearly much smaller than that reported for Cz growth, ≈ 1, [48] or 0.86. [49] The reason for this discrepancy is yet not clear.

Table 1. LFZ experimental growth conditions and crystal compositions. Ø= rod diameter. ν= pulling rate. LP= CO_2 laser power. The rotation rate was 5 rpm in all cases.

Sample	RE_2SiO_5 formula		ø	1st ν	1st LP	2nd ν	2nd LP
	RE nominal	RE in crystal	(mm)	(mm/h)	(W)	(mm/h)	(W)
Nd:LGSO	$Lu_{0.275}Gd_{0.675}Nd_{0.05}$	$Lu_{0.307}Gd_{0.612}Nd_{0.081}$	~2	100	86	10	83
Yb:LGSO	$Lu_{0.275}Gd_{0.675}Yb_{0.05}$	$Lu_{0.351}Gd_{0.630}Yb_{0.019}$	~2	100	88	10	83

3.2 Crystallographic characterization

Figure 3 shows the RT θ-2θ scans of powdered LFZ grown Yb- or Nd-doped LGSO crystals. For the sake of clarity only the region from 2θ= 5 to 55 degrees is presented. Despite manual grinding of the crystalline rods, diffractograms still show a preferential orientation as a consequence of their single-crystalline nature. In both cases the presence of a single phase with *C*2/*c* crystal symmetry is obvious from the comparison with the 2θ peak positions of the ICSD 279584 card corresponding to Lu_2SiO_5.[50] The presence of $P2_1/c$ phase contribution characteristic of Gd_2SiO_5 compound is completely discarded due to the absence of any reflection at 2θ= 10.17 degrees and by the absence of any other 2θ X-ray reflection characteristic of this phase. The single phase character of the LFZ grown ≈0.3Lu/0.7Gd LGSO crystals was in fact previously confirmed by Raman spectroscopy.[42]

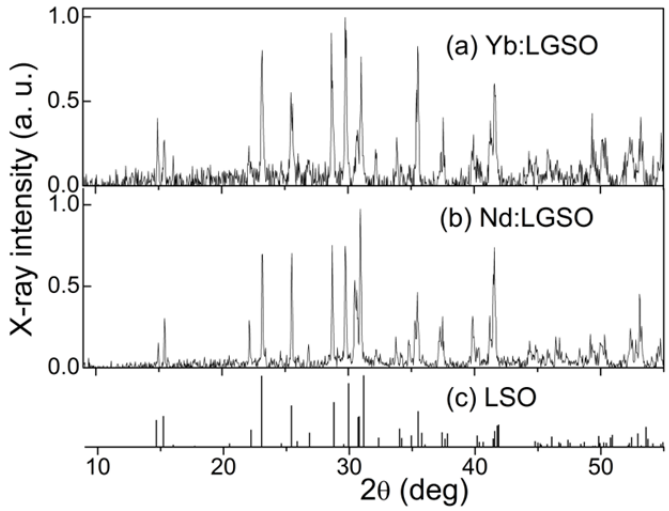

Figure 3. pXRD patterns of grinded $(Lu_{0.351}Gd_{0.630}Yb_{0.019})_2SiO_5$ (a) and $(Lu_{0.307}Gd_{0.612}Nd_{0.081})_2SiO_5$ (b) LFZ grown single-crystals and comparison with the pattern of isostructural Lu_2SiO_5, ICSD cc Nº 279584 (c).

3.3. Laser operation

Yb:LGSO

Two LFZ grown $(Lu_{0.351}Gd_{0.630}Yb_{0.019})_2SiO_5$ crystals with polished parallel faces and thickness d= 1.050 mm and 1.454 mm, respectively, were prepared for laser demonstration. Figure 4 shows the optical absorption of the used pump beam ($^2F_{7/2}\rightarrow{}^2F_{5/2}$ Yb^{3+} transition at λ= 977.8 nm) in these samples under lasing and non lasing conditions. It must be first noted the large difference of absorption in these two regimes, which is typically observed for Yb^{3+} due to its quasi-three

level operation scheme. Under non lasing conditions the crystal absorption at the pumping wavelength decreases due to the deplection of the electronic population of the fundamental $^2F_{7/2}$ multiplet, i.e. a significant fraction of the total electronic population under dark conditions is promoted to the excited $^2F_{5/2}$ multiplet. Under laser action, stimulated $^2F_{5/2} \rightarrow ^2F_{7/2}$ transitions recover the electronic population of the fundamental level and thus the optical absorption is larger than under non lasing conditions. On the other hand the pump optical absorption is always lower than 60%. Such low absorption is associated to the lower than desired content of Yb in the LFZ used crystals (1.86 mol%).

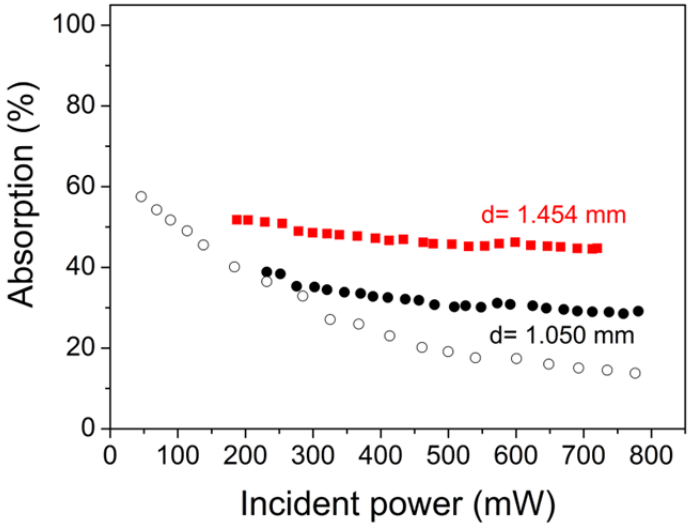

Figure 4. Optical absorption of the λ= 977.8 nm pumping wave in two LFZ grown $(Lu_{0.351}Gd_{0.630}Yb_{0.019})_2SiO_5$ crystals under lasing (full symbols) and not lasing (open symbols) conditions for increasing incident pump power. Black circles correspond to d= 1.050 mm sample thickness and red squares to the d= 1.454 mm one.

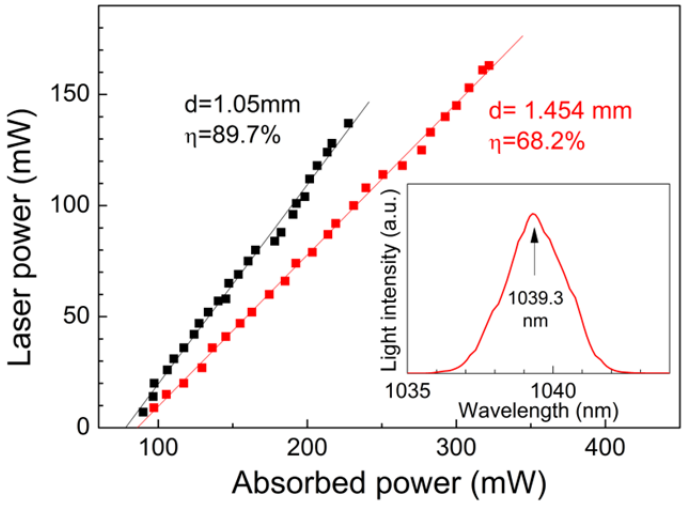

Figure 5. Input-output cw laser power characteristics of two LFZ grown $(Lu_{0.351}Gd_{0.630}Yb_{0.019})_2SiO_5$ crystals with thickness 1.050 mm (black symbols) and 1.454 mm (red symbols) under Tisa pumping at λ= 977.8 nm (T_{OC}= 10%). The symbols are the experimental results and the lines are the linear fits used for the calculation of the laser slope efficiencies. The inset shows the spectral distribution of the laser emission of the 1.454 mm thick sample with maximum at λ= 1039.3 nm and a FWHM= 2.4 nm.

Stable cw laser emission was obtained in both samples under Tisa excitation at λ= 977.8 nm. Figure 5 shows the results obtained for both studied samples. The thinner sample, d= 1.050 mm, showed the highest slope efficiency η= 89.7% and lowest pump threshold P_{th}= 78 mW. While these values are slightly worse for the d= 1.454 mm sample (η= 68.2%, P_{th}= 82 mW) the maximum output power obtained, 164 mW, was higher due to the larger optical absorption of this sample, see Figure 4. The output emission of the thicker sample was rather unpolarized and quite stable with a maximum at λ= 1039. 3 nm and a full width at half maximum FWHM= 2.4 nm. The thinner sample also showed a weak polarization character but its free running emission jumps from λ= 1006 nm to λ= 1038 nm depending of the cavity alignment and often shows a dual wavelength emission.

Table 2. Comparison of cw laser performance of LFZ and Cz grown Yb-doped oxyorthosilicates. GM=Growth method. Ø=pump beam waist diameter. L=sample thickness. Pol=Pumping polarization respect crystalline structure. P_{th}=absorbed pump power threshold. η=laser slope efficiency versus absorbed power. P_{MAX}=maximum output laser power. ?=unknown.

GM	Crystal composition	L (mm)	Cavity,laser, Ø (μm)	λ_{PUMP}/ λ_{EMI} (nm/nm)	Pol	P_{th} (W)	η (%)	P_{MAX} (W)	Reference
LFZ	$(Lu_{0.351}Gd_{0.630}Yb_{0.019})SO$	1.050 1.454	Z,Tisa,62	977.8/1039.3	?	0.078 0.082	89 68	0.137 0.164	This Work
Cz	$Yb:(Gd_{0.5}Y_{0.5})SO$	2	V,DL,50	974/1058	?	0.4	79	2.3	[33]
Cz	5%Yb:LuYSO	2	V,DL,50 V,DL,400	976/1086	?	1.1 3.9	85 64	2.1 7.8	[32]

Cz	5%Yb:LuSO	3.65
		1.29
		1.29
		3.65
			V,DL,140	969/?	b//X
					//Y
					//Z
					//Z
						0.8
						0.3
						0.5
						0.8
							64
							80
							70
							62
								4.5
								2.1
								2.0
								5.0
									[51]

Cz	$5\%Yb:(Gd_{0.5}Y_{0.5})SO$	3	V,DL,200	977/1081.5	?	1.2	57	2.44	[31]
Cz	5%Yb:YSO	2	V,DL,200	978/1082	//X	1	67	7.7	[25]
Cz	8%Yb:LuSO	2	V,DL,200	978/1058	//X	1.1	62	7.3	[25]
Cz	$5\%Yb:(Gd_{0.1}Y_{0.9})SO$	2.8	PC,DL,400	936/1080	?	6	18	0.958	[34]

Table 2 compares the laser efficiency of LFZ Yb:LGSO crystals with those obtained for isostructural Cz-grown single-crystals.[25,41-44,51] Considering exclusively the results of Cz-grown crystals it is obvious that large slope efficiencies and small pumping thresholds are directly related to small pumping beam waist, while for large output power the pumping source must be powerful, implying the use of a large beam waist to avoid crystal damage. The comparison of these results is not straightforward because in some cases the crystal orientation is unknown. Nevertheless, to the light of these considerations, the laser performance of the LFZ Yb:LGSO crystals here presented must be considered equivalent to that of Cz-grown crystals. Laser slope efficiency as large as the best reported for Cz-grown 5mol%Yb:LSO [32] have been obtained and the laser thresholds in LFZ crystals are significantly lower than those of Cz-grown counterparts, of course the high Gaussian beam quality of the Tisa laser helps for this. Certainly the maximum output power here presented for the LFZ crystals are moderate, but this is related to the low Yb concentration used (1.86 mol%) leading to low pump absorption (see Figure 4) and short sample thickness, as well as to the available pump power of the used Tisa laser (<1.2 W at λ= 977.3 nm) in comparison to DL pumping sources with power in excess of 10 W.

Nd:LGSO

A polished parallel faces $(Lu_{0.307}Gd_{0.612}Nd_{0.081})_2SiO_5$ sample with a thickness d= 1.272 mm was prepared for laser demonstration. The optimum pumping was found at λ= 811.3 nm, i.e. $^4I_{9/2}\rightarrow{}^4F_{5/2}$ Nd^{3+} absorption. The sample growth axis was set parallel to the horizontal Tisa polarization. Figure 6 shows the sample absorption under lasing and non lasing conditions. Little differences are found between both regimes. In fact this is expected from the 4-level dynamic of the Nd^{3+} ≈ 1.06 μm laser channel (emission through the $^4F_{3/2}\rightarrow{}^4I_{11/2}$ transition). In the non lasing regimen the absorption decreases from ≈ 90% at low pumping power to ≈ 71% at the maximum available Tisa pumping power, which is associated to the depletion of the $^4I_{9/2}$ electronic population. This bleaching is slightly recovered under lasing conditions and the final absorption in the bleached state remains at 75%.

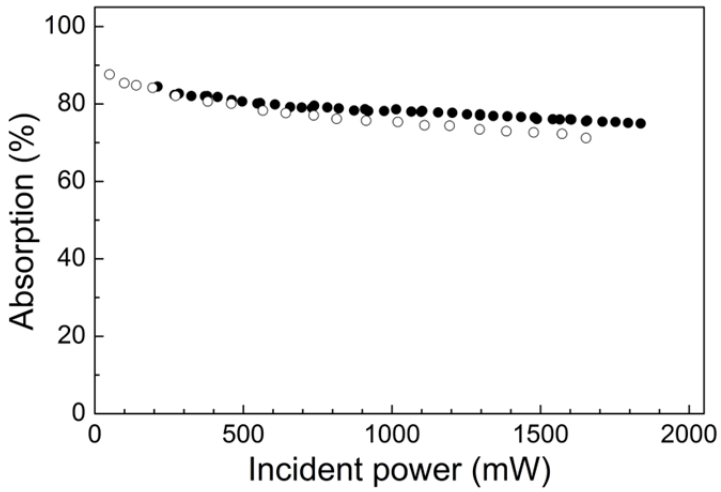

Figure 6. Optical absorption of the λ= 811.3 nm pumping wave in a LFZ grown $(Lu_{0.307}Gd_{0.612}Nd_{0.081})_2SiO_5$ crystal under lasing (full symbols) and not lasing (open symbols) conditions for increasing incident pump power.

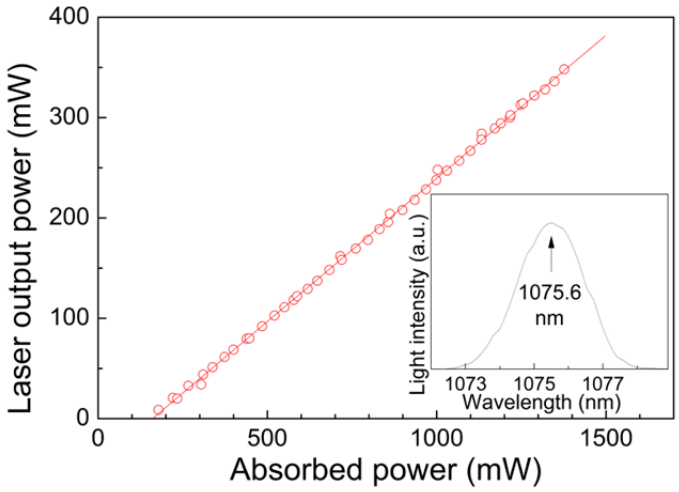

Figure 7. Input-output quasi-cw laser power characteristics of a LFZ grown $(Lu_{0.307}Gd_{0.612}Nd_{0.081})_2SiO_5$ crystal with thickness 1.272 mm under Tisa pumping at λ= 811.3 nm (T_{OC}= 10%). The symbols are the experimental results and the line is the linear fit used for the calculation of the laser slope efficiency. The inset shows the spectral distribution of the laser emission with maximum at λ= 1075.6 nm and a FWHM= 2.3 nm.

Laser emission was observed in cw regime but the output power was unstable likely due to local heating of the sample associated to the relatively high Nd concentration used in this work (8.06 mol%). This was alleviated by chopping the pump beam with a 50% duty cycle factor in a quasi-continuous wave (qcw) mode. Figure 7 shows the input-output laser power characteristic of the tested Nd:LGSO LFZ crystal. The laser emission was centered at λ=1075.6 nm with a FWHM= 2.3 nm, see Fig. 7 inset. The pump power threshold was only 160 mW and the laser slope efficiency (versus absorbed power) was η= 28.5%. It is worth noting that the laser emission wavelength is significantly larger than that observed in Nd:YAG (typically λ≈ 1060 nm), that is associated to the above mentioned large crystal field characteristic of oxyorthosilicates.

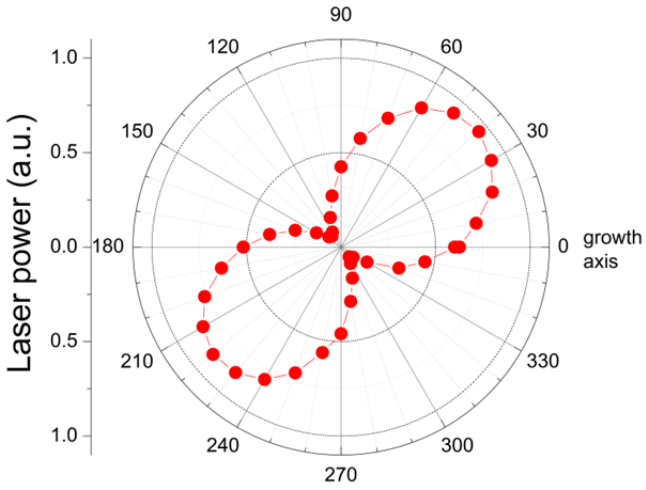

Figure 8. Polar plot of the laser power emitted by a LFZ grown $(Lu_{0.307}Gd_{0.612}Nd_{0.081})_2SiO_5$ crystal at different angles with regards to the rod growth axis. The symbols are the experimental results and the line the fit to a $\cos^2$ law.

By inserting a polarizer at the resonator output, the laser emission was observed to be linearly polarized. Figure 8 shows the relative laser output power for different angles with respect to the sample growth axis. Maximum power is obtained at about 40 degree off the rod growth axis. Since the sample was set normal to the pumping beam this polarization must be ascribed to spatial variations of the Nd^{3+} emission cross section (σ_{EMI}). The anisotropy of the Nd^{3+} spectroscopy was studied in detail by Beach et al. in Nd:YSO Cz-grown single-crystal. [45] It was shown that along the indicatrix X-axis (taken parallel to the 2-fold crystallographic b-axis) σ_{EMI} is larger than for the two other indicatrix axes (named as Y and Z) however the accuracy of the reported data does not allow a precise evaluation of the differences at our λ= 1075.6 nm laser emission wavelength. Nevertheless, from the results of Figure 8 it seems to us likely that the crystallographic b-axis of the sample is contained in a plane which is tilted about 40 degree off the fiber growth axis.

The laser efficiency performance obtained for LFZ Nd-doped crystal can be compared with that previously reported in Cz-grown single-crystals, however this comparison must be taken with care due to the experimental differences, such as Nd concentration, crystal length/absorption, used optical cavity design or pumping conditions. To our knowledge, all previous lasing reports of Nd-doped isostructural oxyorthosilicates have been done pumping with DL and pumping beam waist diameters are larger than in our case. Table 3 summarizes a comparison of laser performance of Cz-grown crystals and those grown by LFZ. Borel et al. [28] used a plane-concave cavity and focused an AlGaAs DL beam to a 130 μm waist diameter, which is not very far from our experimental conditions. They obtained a maximum output power of only 260 mW (versus our 350 mW) but the slope efficiency was higher than in our case. This difference is most likely due to the different crystal orientation, that in our case was not optimized parallel to the crystalline b-axis and to the higher Nd concentration used by us which advance large non radiative Nd fluorescence losses. Higher laser output power (up to 444 mW) has been demonstrated by Li et al.,[29] but the pump threshold and the slope efficiency are much higher/lower, respectively, than those obtained here for the studied LFZ Nd-doped LGSO crystal.

Table 3. Comparison of laser performance of LFZ and Cz grown oxyorthosilicate crystals doped with Nd. GM=Growth method. Ø=pump beam waist diameter. L=sample thickness. Pol=Pumping polarization. P_{th}=absorbed pump power threshold. η=laser slope efficiency versus absorbed power. P_{MAX}=maximum output laser power. ?=unknown.

GM	Crystal composition	L (mm)	Cavity,laser, Ø --, --, (μm)	$\lambda_{PUMP}/\lambda_{EMI}$ (nm/nm)	Pol	P_{th} (W)	η (%)	P_{MAX} (W)	Reference
LFZ	$(Lu_{0.307}Gd_{0.612}Nd_{0.081})SO$	1.272	Z, Tisa, 62	811.3/1075.6	?	0.160	28.5	0.350	This work
Cz	1mol%Nd:YSO	5	PC, DL, 130	810/ ?	//X //Z	0.069 0.080	54 48	0.260 0.200	[28]
Cz	$(Lu_{0.4975}Gd_{0.4975}Nd_{0.005})SO$	5.5	PC, DL, ?	811/ ?	?	3.13	17.7	0.444	[29]

4. CONCLUSIONS AND FURTHER COMMENTS

Monocrystalline rods with $(Lu_{0.351}Gd_{0.630}Yb_{0.019})_2SiO_5$ and $(Lu_{0.307}Gd_{0.612}Nd_{0.081})_2SiO_5$ compositions were successfully grown in air by means of the Laser Floating Zone (LFZ) method. Key steps for the successful growth of crystals with optical transparency were the use of finely grinded precursors, the selection of the correct Lu/Gd ratio and the use of moderate pulling, 10 mm/h, and rotation, 5 rpm, rates. These crystals exhibit the monoclinic *C*2/*c* crystalline structure, also reported for Lu_2SiO_5 and Y_2SiO_5, which is free of the cleavage observed in the $P2_1/c$ Gd_2SiO_5 oxyorthosilicate. It has been shown that despite the fact that these are the first laser results obtained in a LFZ grown oxyorthosilicate single crystal, the laser performance is comparable to that obtained in established Czochralski (Cz) grown oxyorthosilicate crystals. Further improvements of the laser performance can be expected in the future by a better control of the Nd or Yb laser ions composition in the oxyorthosilicate host, by a more controlled crystal orientation and by using DL pumping for laser demonstration.

Although laser operation has been obtained in both LFZ grown Yb- or Nd-doped oxyorthosilicates, the presence of transversal cracks in the latter definitely limits some laser applications, particularly the desirable DL pumping along the growth axis. Despite some fluctuation, the rod diameters presently obtained (≈ 1.5-1.75 mm) are ideal for high power DL pumping since they support the currently used DL pump beam sizes (≤ 1 mm) while they would allow an efficient lateral cooling, maximizing the surface/volume of the laser element. At the present development state of the used LFZ growth system this seems possible only for the Yb-doped oxyorthosilicate. Although the local crystalline quality of present Nd-doped oxyorthosilicate is suitable for lasing pumping with the highly focused Tisa laser beam, DL pumping would require further crystal growth improvements to eliminate transversal cracks.

The LFZ growth technique has several advantages over Cz growth, such as the high crystal purity inherent to the absence of any crucible, a crystallization rate between one and two orders of magnitude larger and no requirement of controlled growth atmosphere (oxide crystals are grown in air), thus the LFZ technique is a practical, fast, and low cost growth method to produce laser gain media particularly for material with congruent high melting temperature.

ACKNOWLEDGMENTS

This work is funded by FEDER funds (COMPETE 2020 Programme), by national funds through FCT - Portuguese Foundation for Science and Technology (UID/CTM/50025/2019) as well as by Ministerio de Ciencia Innovación y Universidades (RTI2018-094859-B-I00, also FEDER co-fund) of Spain. F. Rey-García acknowledges SPRINT (EU H2020-FET-OPEN/0426), Xunta de Galicia (ED431E 2018/08) and FCT (SFRH/BPD/108581/2015) projects. XRD data collection by C. Cascales is acknowledged. Microprobe compositional analyses have been performed at the Centro Nacional de Microscopía Electrónica of Universidad Complutense de Madrid.

REFERENCES

[1] T. Südmeyer, C. Kränkel, C. R. E. Baer, O. H. Heckl, C. J. Saraceno, M. Golling, R. Peters, K. Petermann, G. Huber and U. Keller, *Appl. Phys. B*, 2009, **97**, 281.
[2] A. J. Kemp, G. J. Valentine and D. Burns, *Progress in Quantum Electronics*, 2004, **28**, 305.
[3] B. Weichelt, K. S. Wentsch, A. Voss, M. A. Ahmed and Th. Graf, *Laser Phys. Lett.*, 2012, **9**, 110.
[4] S. M. Koohpayeh, D. Fort and J. S. Abell, *Progress in Crystal Growth and Characterization of Materials*, 2008, **54**, 121.
[5] M. R. B. Andreeta and A. C. Hernandes, Springer Handbook of Crystal Growth. Editors G. Dhanaraj, K . Byrappa, V. Prasad and M. Dudley. Berlin, Springer; p. 393-432, 2010.
[6] J. Stone, C. A. Burrus, A. G. Dentai and B. I. Miller, *Appl. Phys. Lett.*, 1976, **29**, 37.
[7] J. Stone and C. A. Burrus, *J. Appl. Phys.*, 1978, **49**, 2281.
[8] G. F. de la Fuente, L. R. Black, D. M. Andrauskas and H. R. Verdún, *Sol. St. Ionics*, 1989, **32/33**, 494.
[9] L. R. Black, D. M. Andrauskas, G. F. de la Fuente and H. R. Verdún, *Proceedings SPIE 1104 Growth, Characterization, and Applications of Laser Host and Nonlinear Crystals*, 1989, **1104**, 175.
[10] B. M. Tissue, L. Lu, L. Ma, W. Jia, M. L. Norton and W. M. Yen, *J. Cryst. Growth* 1991, **109**, 323.
[11] S. Erdei and F. W. Ainger, *J. Cryst. Growth*, 1993, **128**, 1025.
[12] T. Ogawa, Y. Urata, S. Wada, K. Onodera, H. Machida, H. Sagae, M. Higuchi and K. Kodaira, *Opt. Lett.*, 2003, **28**, 2333.
[13] X. Yan, X. Wu, J. Zhou, Z. Zhang and J. Wang, *J. Cryst. Growth*, 2000, **220**, 543.
[14] R. Lisiecki, P. Solarz, G. Dominiak-Dzik, W. Ryba-Romanowski, M. Sobczyk, P. Černý, J. Šulc, H. Jelínková, Y. Urata and M. Higuchi, *Phys. Rev. B*, 2006, **74**, 035103.
[15] S. Nakamura, T. Agata, T. Ogawa, S. Wada and M. Higuchi, *Opt. Rev.*, 2013, **20**, 390.
[16] J. J. Romero, E. Montoya, L. E. Bausá, F. Agulló-Rueda, M. R. B. Andreeta and A. C. Hernandes, *Opt. Mater.*, 2004, **24**, 643.
[17] Y. Sato and T. Taira, *Opt. Express*, 2006, **14**,10528.
[18] R. L. Aggarwal, D. J. Ripin, J. R. Ochoa and T. Y. Fan, *J. Appl. Phys.*, 2005, **98**, 103514.
[19] R. Gaumé, B. Viana, D. Vivien, J. Roger and D. Fournier, *Appl. Phys. Lett.*, 2003, **83**, 1355.
[20] M. Jie, G. Zhao, X. Zeng, L. Su, H. Pang, X. He and J. Xu, *J. Cryst. Growth*, 2005, **277**, 175.
[21] W. Li, H. Pan. L. Ding, H. Zeng, G. Zhao, C. Yan, L. Su and J. Xu, *Opt. Express*, 2006, **14**, 686.
[22] W. Li, Q. Hao, H. Zhai, H. Zeng, W. Lu, G. Zhao, L. Zheng, L. Su and J. Xu, *Opt. Express*, 2007, **15**, 2354.
[23] C. Li, R. Moncorgé, J. C. Souriau and Ch. Wyon, *Opt. Comm.*, 1993, **101**, 356.
[24] L. Zheng, J. Xu, L. Su, H. Li, W. Ryba-Romanowski, R. Lisiecki and P. Solarz, *Appl. Phys. Lett.*, 2010, **96**, 121908.
[25] M. Jacquemet, C. Jacquemet, N. Janel, F. Druon, F. Balembois, P. Georges, J. Petit, B. Viana, D. Vivien and B. Ferrand, *Appl. Phys. B*, 2005, **80**, 171.
[26] R. Gaume, P. H. Haumesser, B. Viana, D. Vivien, B. Ferrand and G. Aka, *Opt. Mater.*, 2002, **19**, 81.
[27] H. Cong, H. Zhang, J. Wang, W. Yu, J. Fan, X. Cheng, S. Sun, J. Zhang, Q. Lu, C. Jiang and R. I. Boughton, *J. Appl. Cryst.*, 2009, **42**, 284.
[28] C. Borel, N. Herlet, R. Templier, C. Calvat and C. Wyon, *J. de Physique IV France*, 1994, **4**, C4-549.
[29] D. Z. Li, X. D. Xu, J. Zhang, Z. H. Cong, D. Y. Tang, J. Ma, H. M. Zhu, X. Y. Chen, F. Wu, C. T. Xia and J. Xu, *Laser Phys. Lett.*, 2011, **8**, 647.
[30] X. Guan, Z. Zhou, X. Huang, B. Xu, H. Xu, Z. Cai, X. Xu, D. Li and J. Xu, *Laser Phys.*, 2017, **27**, 125806.
[31] J. Du, X. Liang, Y. Xu, R. Li, Z. Xu, C. Yan, G. Zhao, L. Su and J. Xu, *Opt. Express*, 2006, **14**, 3333.
[32] W. Li, S. Xu, H. Pan, L. Ding, H. Zeng, W. Lu, C. Guo, G. Zhao, C. Yan, L. Su and J. Xu, *Opt. Express*, 2006, **14**, 6681.
[33] W. Li, Q. Hao, L. Ding, G. Zhao, L. Zheng, J. Xu and H. Zeng, *IEEE J. Quantum Electron.*, 2008, **44**, 567.
[34] H. Chu, S. Zhao, K. Yang, J. Zhao, D. Li, G. Li, T. Li, W. Qiao, X. Xu, L. Zheng and J. Xu, *Opt. Mater.*, 2015, **45**, 181.
[35] T. Wen-Long, W. Zhao-Hua, Z. Jiang-Feng, W. Zhi-Yi, Z. Li-He, X. Xiao-Dong and X. Jun, *Chin. Phys. Lett.*, 2015, **32**, 024206.
[36] F. Thibault, D. Pelenc, F. Druon, Y. Zaouter, M. Jacquemet and P. Georges, *Opt. Lett.*, 2006, **31**, 1555.
[37] D. W. Cooke, R. E. Muenchausen, K. J. McClellan and B. L. Bennett, *Opt. Mater.*, 2005, **27**, 1781.
[38] H. Farhi, K. Lebbou, S. Belkahla, L. Grosvalet, B. Hautefeuille, A. Caramanian, C. Dujardin, O. Tillement and C. Pedrini, *Opt. Mater.*, 2008, **30**, 1461.

[39] F. Rey-García, N. Ben Sedrine, J. Rodrigues, N. M. Ferreira, A. J. S. Fernandes, T. Monteiro and F. M. Costa, *Abstract book of I Iberian Meeting on Materials Science, Salamanca (Spain)* 2018.
[40] F. Rey-García, N. B. Sedrine, M. R. Soares, A. J. S. Fernandes, A. B. Lopes, N. M. Ferreira, T. Monteiro and F. M. Costa, *Opt. Mater. Express*, 2017, **7**, 868.
[41] F. Rey-García, N. B. Sedrine, A. J. S. Fernandes, T. Monteiro and F. M. Costa, *J. Eur Cer. Soc.*, 2018, **38**, 2059.
[42] F. Rey-García, A. J. S. Fernandes and F. M. Costa, Mater. Res. Bull., 2019, **112**, 413.
[43] F. Rey-García, J. Rodrigues, A. J. S. Fernandes, M. R. Soares, T. Monteiro and F. M. Costa, *CrystEngComm*, 2018, **20**, 7386.
[44] E. Castellano-Hernández, X. Han, M. Rico, L. Roso, C. Cascales and C. Zaldo, *Opt. Express*, 2019, **23**, 11135.
[45] R. Beach, M. D. Shinn, L. Davis, R. W. Solarz and W. F. Krupke, *IEEE J. Quantum Electron.*, 1990, **26**, 1405.
[46] G. E. Jellison, Jr., E. D. Specht, L. A. Boatner, D. J. Singh and C. L. Melcher, *J. Appl. Phys.*, 2012, 112, 063524.
[47] E. V. Zharikov, C. Zaldo and F. Díaz, MRS Bulletin, 2009, 34, 271.
[48] P. Haumesser, R. Gaumé, J. Benitez, B. Viana, B. Ferrand, G. Aka and D. Vivien, *J. Cryst. Growth*, 2001, **233**, 233.
[49] C. Yan, G. Zhao, L. Su, X. Xu, L. Zhang and J. Xu, *J. Phys. Condens. Matter*, 2006, **18**, 1325.
[50] T. Gustafsson, M. Klintenberg, S. E. Derenzo, M. J. Weber and J. O. Thomas, *Acta Cryst.*, 2001, **C57**, 668.
[51] G. Toci, A. Pirri, A. Beitlerova, Y. Shoji, A. Yoshikawa, J. Hybler, M. Nikl and M. Vannini, *Opt. Express*, 2015, **23**, 13210.